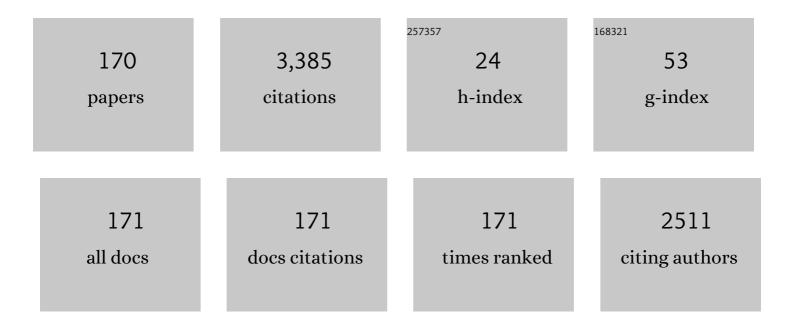
Giovanni Verzellesi

List of Publications by Year in descending order

Source: https://exaly.com/author-pdf/368751/publications.pdf Version: 2024-02-01



#	Article	IF	CITATIONS
1	Role of carbon in dynamic effects and reliability of 0.15-um AlGaN/GaN HEMTs for RF power amplifiers. , 2022, , .		1
2	Failure Physics and Reliability of GaNâ€Based HEMTs for Microwave and Millimeterâ€Wave Applications: A Review of Consolidated Data and Recent Results. Physica Status Solidi (A) Applications and Materials Science, 2022, 219, .	0.8	6
3	Testing of planar hydrogenated amorphous silicon sensors with charge selective contacts for the construction of 3D-detectors. Journal of Instrumentation, 2022, 17, C03033.	0.5	3
4	Defects in III-N LEDs: experimental identification and impact on electro-optical characteristics. , 2022, ,		0
5	Editorial for the Special Issue on Wide Bandgap Based Devices: Design, Fabrication and Applications, Volume II. Micromachines, 2022, 13, 403.	1.4	0
6	Deep defects in InGaN LEDs: modeling the impact on the electrical characteristics. , 2022, , .		0
7	Experimental and numerical investigation of Poole–Frenkel effect on dynamic R _{ON} transients in C-doped p-GaN HEMTs. Semiconductor Science and Technology, 2022, 37, 025006.	1.0	6
8	"Hole Redistribution―Model Explaining the Thermally Activated <i>R</i> _{ON} Stress/Recovery Transients in Carbon-Doped AlGaN/GaN Power MIS-HEMTs. IEEE Transactions on Electron Devices, 2021, 68, 697-703.	1.6	36
9	Evaluation of VTH and RON Drifts during Switch-Mode Operation in Packaged SiC MOSFETs. Electronics (Switzerland), 2021, 10, 441.	1.8	10
10	Mechanisms Underlying the Bidirectional <i>V</i> _T Shift After Negative-Bias Temperature Instability Stress in Carbon-Doped Fully Recessed AlGaN/GaN MIS-HEMTs. IEEE Transactions on Electron Devices, 2021, 68, 2564-2567.	1.6	10
11	On the Modeling of the Donor/Acceptor Compensation Ratio in Carbon-Doped GaN to Univocally Reproduce Breakdown Voltage and Current Collapse in Lateral GaN Power HEMTs. Micromachines, 2021, 12, 709.	1.4	8
12	Modeling the electrical characteristics of InGaN/GaN LED structures based on experimentally-measured defect characteristics. Journal Physics D: Applied Physics, 2021, 54, 425105.	1.3	21
13	Partial Recovery of Dynamic <i>R</i> _{ON} Versus OFF-State Stress Voltage in p-GaN Gate AlGaN/GaN Power HEMTs. IEEE Transactions on Electron Devices, 2021, 68, 4862-4868.	1.6	24
14	Fabrication of a Hydrogenated Amorphous Silicon Detector in 3-D Geometry and Preliminary Test on Planar Prototypes. Instruments, 2021, 5, 32.	0.8	8
15	GaN-based power devices: Physics, reliability, and perspectives. Journal of Applied Physics, 2021, 130, .	1.1	191
16	The Role of Carbon Doping on Breakdown, Current Collapse, and Dynamic Onâ€Resistance Recovery in AlGaN/GaN High Electron Mobility Transistors on Semiâ€Insulating SiC Substrates. Physica Status Solidi (A) Applications and Materials Science, 2020, 217, 1900762.	0.8	14
17	Characterization of a premixed flat combustor through plasma current measurements. , 2020, , .		0
18	Characterization and TCAD Modeling of Mixed-Mode Stress Induced by Impact Ionization in Scaled SiGe HBTs. IEEE Transactions on Electron Devices, 2020, 67, 4597-4601.	1.6	1

#	Article	IF	CITATIONS
19	The effects of carbon on the bidirectional threshold voltage instabilities induced by negative gate bias stress in GaN MIS-HEMTs. Journal of Computational Electronics, 2020, 19, 1555-1563.	1.3	16
20	Hydrogenated amorphous silicon detectors for particle detection, beam flux monitoring and dosimetry in high-dose radiation environment. Journal of Instrumentation, 2020, 15, C04005-C04005.	0.5	4
21	Modeling a Thick Hydrogenated Amorphous Silicon Substrate for Ionizing Radiation Detectors. Frontiers in Physics, 2020, 8, .	1.0	6
22	Systematic Modeling of Electrostatics, Transport, and Statistical Variability Effects of Interface Traps in End-of-the-Roadmap III–V MOSFETs. IEEE Transactions on Electron Devices, 2020, 67, 1560-1566.	1.6	2
23	Trap Dynamics Model Explaining the R _{ON} Stress/Recovery Behavior in Carbon-Doped Power AlGaN/GaN MOS-HEMTs. , 2020, , .		11
24	Effects of mole fraction variations and scaling on total variability in InGaAs MOSFETs. Solid-State Electronics, 2019, 159, 135-141.	0.8	3
25	On the impact of channel compositional variations on total threshold voltage variability in nanoscale InGaAs MOSFETs. , 2018, , .		2
26	Physical mechanisms limiting the performance and the reliability of GaN-based LEDs. , 2018, , 455-489.		9
27	Electrical leakage phenomenon in heteroepitaxial cubic silicon carbide on silicon. Journal of Applied Physics, 2018, 123, .	1.1	13
28	A Wireless Personal Sensor Node for Real Time Dosimetry of Interventional Radiology Operators. Lecture Notes in Electrical Engineering, 2017, , 1-7.	0.3	1
29	A novel test methodology for R <inf>ON</inf> and V <inf>TH</inf> monitoring in GaN HEMTs during switch-mode operation. , 2017, , .		0
30	Comprehensive Capacitance–Voltage Simulation and Extraction Tool Including Quantum Effects for High-k on Si <italic>x</italic> Ge1â^' <italic>x</italic> and In <italic>x</italic> Ga1â^' <italic>x</italic> As: Part l—Model Description and Validation. IEEE Transactions on Electron Devices, 2017, 64, 3786-3793.	1.6	3
31	Comprehensive Capacitance–Voltage Simulation and Extraction Tool Including Quantum Effects for High- \$k\$ on SixGe1â^'x and InxGa1â^'xAs: Part Il—Fits and Extraction From Experimental Data. IEEE Transactions on Electron Devices, 2017, 64, 3794-3801.	1.6	4
32	Combined variability/sensitivity analysis in III-V and silicon FETs for future technological nodes. , 2017, , .		4
33	Modelling of GaN HEMTs: From Device-Level Simulation to Virtual Prototyping. Power Electronics and Power Systems, 2017, , 165-196.	0.6	2
34	The impact of interface and border traps on current–voltage, capacitance–voltage, and split V mobility measurements in InGaAs MOSFETs. Physica Status Solidi (A) Applications and Materials Science, 2017, 214, 1600592.	0.8	12
35	Modelling nanoscale n-MOSFETs with III-V compound semiconductor channels: From advanced models for band structures, electrostatics and transport to TCAD. , 2017, , .		9
36	Variability and sensitivity to process parameters variations in InGaAs dual-gate ultra-thin body MOSFETs: A scaling perspective. , 2017, , .		1

#	Article	IF	CITATIONS
37	Threshold Voltage Statistical Variability and Its Sensitivity to Critical Geometrical Parameters in Ultrascaled InGaAs and Silicon FETs. IEEE Transactions on Electron Devices, 2017, 64, 4607-4614.	1.6	12
38	Random dopant fluctuation variability in scaled InGaAs dual-gate ultra-thin body MOSFETs: Source and drain doping effect. , 2017, , .		1
39	The PixFEL front-end for X-ray imaging in the radiation environment of next generation FELs. , 2017, , .		Ο
40	A pixelated x-ray detector for diffraction imaging at next-generation high-rate FEL sources. , 2017, , .		2
41	PFM2: a 32 × 32 processor for X-ray diffraction imaging at FELs. Journal of Instrumentation, 2016, 11, C11033-C11033.	0.5	Ο
42	Effects of border traps on transfer curve hysteresis and split-CV mobility measurement in InGaAs quantum-well MOSFETs. , 2016, , .		0
43	A 2D imager for X-ray FELs with a 65 nm CMOS readout based on per-pixel signal compression and 10 bit A/D conversion. Nuclear Instruments and Methods in Physics Research, Section A: Accelerators, Spectrometers, Detectors and Associated Equipment, 2016, 831, 301-308.	0.7	6
44	Experimental and Numerical Analysis of Hole Emission Process From Carbon-Related Traps in GaN Buffer Layers. IEEE Transactions on Electron Devices, 2016, 63, 3473-3478.	1.6	76
45	Correlation between dynamic Rdsou transients and Carbon related buffer traps in AlGaN/GaN <code>HEMTs.</code> , 2016, , .		12
46	PFM2: A 32 $ ilde{A}$ — 32 readout chip for the PixFEL X-ray imager demonstrator. , 2016, , .		1
47	First experimental results on active and slim-edge silicon sensors for XFEL. Journal of Instrumentation, 2016, 11, C12018-C12018.	0.5	1
48	The PixFEL project: Progress towards a fine pitch X-ray imaging camera for next generation FEL facilities. Nuclear Instruments and Methods in Physics Research, Section A: Accelerators, Spectrometers, Detectors and Associated Equipment, 2016, 824, 131-134.	0.7	0
49	In-pixel conversion with a 10 bit SAR ADC for next generation X-ray FELs. Nuclear Instruments and Methods in Physics Research, Section A: Accelerators, Spectrometers, Detectors and Associated Equipment, 2016, 824, 313-315.	0.7	4
50	Challenges towards the simulation of GaN-based LEDs beyond the semiclassical framework. Proceedings of SPIE, 2016, , .	0.8	6
51	Design and TCAD simulation of planar p-on-n active-edge pixel sensors for the next generation of FELs. Nuclear Instruments and Methods in Physics Research, Section A: Accelerators, Spectrometers, Detectors and Associated Equipment, 2016, 824, 384-385.	0.7	6
52	Defect-related tunneling contributions to subthreshold forward current in GaN-Based LEDs. , 2015, , .		0
53	A 10 bit resolution readout channel with dynamic range compression for X-ray imaging at FELs. , 2015, , \cdot		0
54	Physicsâ€based modeling and experimental implications of trapâ€assisted tunneling in InGaN/GaN lightâ€emitting diodes. Physica Status Solidi (A) Applications and Materials Science, 2015, 212, 947-953.	0.8	77

#	Article	IF	CITATIONS
55	Extraction of interface state density in oxide/III–V gate stacks. Semiconductor Science and Technology, 2015, 30, 065013.	1.0	7
56	Off-state breakdown characteristics of AlGaN/GaN MIS-HEMTs for switching power applications. , 2015, , .		4
57	Semiclassical simulation of trap-assisted tunneling in GaN-based light-emitting diodes. Journal of Computational Electronics, 2015, 14, 444-455.	1.3	34
58	Analysis of off-state leakage mechanisms in GaN-based MIS-HEMTs: Experimental data and numerical simulation. Solid-State Electronics, 2015, 113, 9-14.	0.8	7
59	The PixFEL project: development of advanced X-ray pixel detectors for application at future FEL facilities. Journal of Instrumentation, 2015, 10, C02024-C02024.	0.5	13
60	PixFEL: developing a fine pitch, fast 2D X-ray imager for the next generation X-FELs. Nuclear Instruments and Methods in Physics Research, Section A: Accelerators, Spectrometers, Detectors and Associated Equipment, 2015, 796, 2-7.	0.7	10
61	Trap-assisted tunneling contributions to subthreshold forward current in InGaN/GaN light-emitting diodes. , 2015, , .		2
62	Modeling challenges for high-efficiency visible light-emitting diodes. , 2015, , .		3
63	Breakdown investigation in GaN-based MIS-HEMT devices. , 2014, , .		7
64	Trapping and high field related issues in GaN power HEMTs. , 2014, , .		15
65	Trap-assisted tunneling in InGaN/GaN LEDs: Experiments and physics-based simulation. , 2014, , .		12
66	ESD degradation and robustness of RGB LEDs and modules: An investigation based on combined electrical and optical measurements. Microelectronics Reliability, 2014, 54, 1143-1149.	0.9	3
67	Threshold voltage instabilities in D-mode GaN HEMTs for power switching applications. , 2014, , .		16
68	Influence of Buffer Carbon Doping on Pulse and AC Behavior of Insulated-Gate Field-Plated Power AlGaN/GaN HEMTs. IEEE Electron Device Letters, 2014, 35, 443-445.	2.2	90
69	Correlating electroluminescence characterization and physics-based models of InGaN/GaN LEDs: Pitfalls and open issues. AIP Advances, 2014, 4, .	0.6	29
70	Low-noise readout channel with a novel dynamic signal compression for future X-FEL applications. , 2014, , .		1
71	PixFEL: Enabling technologies, building blocks and architectures for advanced X-ray pixel cameras at the next generation FELs. , 2014, , .		2
72	Design and TCAD simulations of planar active-edge pixel sensors for future XFEL applications. , 2014, , .		4

#	Article	IF	CITATIONS
73	Efficiency droop in InGaN/GaN blue light-emitting diodes: Physical mechanisms and remedies. Journal of Applied Physics, 2013, 114, .	1.1	351
74	Recent developments on CMOS MAPS for the SuperB Silicon Vertex Tracker. Nuclear Instruments and Methods in Physics Research, Section A: Accelerators, Spectrometers, Detectors and Associated Equipment, 2013, 718, 283-287.	0.7	5
75	Functional test of a Radon sensor based on a high-resistivity-silicon BJT detector. Nuclear Instruments and Methods in Physics Research, Section A: Accelerators, Spectrometers, Detectors and Associated Equipment, 2013, 718, 302-304.	0.7	3
76	Advances in the development of pixel detector for the SuperB Silicon Vertex Tracker. Nuclear Instruments and Methods in Physics Research, Section A: Accelerators, Spectrometers, Detectors and Associated Equipment, 2013, 731, 25-30.	0.7	1
77	The front-end chip of the SuperB SVT detector. Nuclear Instruments and Methods in Physics Research, Section A: Accelerators, Spectrometers, Detectors and Associated Equipment, 2013, 718, 180-183.	0.7	3
78	Latest results of the R&D on CMOS MAPS for the Layer0 of the SuperB SVT. Nuclear Instruments and Methods in Physics Research, Section A: Accelerators, Spectrometers, Detectors and Associated Equipment, 2013, 732, 484-487.	0.7	1
79	Beam test results for the SuperB-SVT thin striplet detector. Nuclear Instruments and Methods in Physics Research, Section A: Accelerators, Spectrometers, Detectors and Associated Equipment, 2013, 718, 314-317.	0.7	1
80	Study of dosimetric observables to be used in Active Pixel Sensor based devices for Interventional Radiology applications. , 2013, , .		2
81	Performance of a radon sensor based on a BJT detector on high-resistivity silicon. , 2012, , .		2
82	Engineering Barrier and Buffer Layers in InGaAs Quantum-Well MOSFETs. IEEE Transactions on Electron Devices, 2012, 59, 3651-3654.	1.6	5
83	Errors Limiting Split-\$CV\$ Mobility Extraction Accuracy in Buried-Channel InGaAs MOSFETs. IEEE Transactions on Electron Devices, 2012, 59, 1068-1075.	1.6	25
84	Investigation of Efficiency-Droop Mechanisms in Multi-Quantum-Well InGaN/GaN Blue Light-Emitting Diodes. IEEE Transactions on Electron Devices, 2012, 59, 1402-1409.	1.6	30
85	BJT detector with FPGA-based read-out for alpha particle monitoring. Journal of Instrumentation, 2011, 6, C01051-C01051.	0.5	5
86	Interface-Trap Effects in Inversion-Type Enhancement-Mode \$hbox{InGaAs/ZrO}_{2}\$ N-Channel MOSFETs. IEEE Transactions on Electron Devices, 2011, 58, 107-114.	1.6	7
87	Design and Characterization of Current-Assisted Photonic Demodulators in 0.18- \$muhbox{m}\$ CMOS Technology. IEEE Transactions on Electron Devices, 2011, 58, 1702-1709.	1.6	16
88	BJT detector for α-particle and Radon detection and monitoring. , 2011, , .		2
89	TOF-Range Image Sensor in 0.18Âμm CMOS technology based on Current Assisted Photonic Demodulators. , 2011, , .		0
90	Analysis of current collapse effect in AlGaN/GaN HEMT: Experiments and numerical simulations. Microelectronics Reliability, 2010, 50, 1520-1522.	0.9	23

6

#	Article	IF	CITATIONS
91	Laser and alpha particle characterization of floating-base BJT detector. Nuclear Instruments and Methods in Physics Research, Section A: Accelerators, Spectrometers, Detectors and Associated Equipment, 2010, 617, 593-595.	0.7	5
92	A 2.4-GHz wireless alpha-ray sensor for remote monitoring and spectroscopy. , 2010, , .		2
93	Fabrication of novel high frequency and high breakdown InAlAs-InGaAs <code>pHEMTs.</code> , 2010, , .		1
94	TCAD optimization of field-plated InAlAs-InGaAs HEMTs. , 2010, , .		1
95	A 180-nm CMOS time-of-flight 3-D image sensor. , 2010, , .		0
96	Analysis of interface-trap effects in inversion-type InGaAs/ZrO <inf>2</inf> MOSFETs. , 2010, , .		1
97	False surface-trap signatures induced by buffer traps in AlGaN-GaN HEMTs. , 2009, , .		6
98	A 4096-pixel MAPS device with on-chip data sparsification. Nuclear Instruments and Methods in Physics Research, Section A: Accelerators, Spectrometers, Detectors and Associated Equipment, 2009, 604, 408-411.	0.7	16
99	On-Chip Fast Data Sparsification for a Monolithic 4096-Pixel Device. IEEE Transactions on Nuclear Science, 2009, 56, 1159-1162.	1.2	2
100	Alpha-particle detection based on the BJT detector and simple, IC-based readout electronics. Journal of Instrumentation, 2009, 4, P11010-P11010.	0.5	5
101	Reliability of GaN High-Electron-Mobility Transistors: State of the Art and Perspectives. IEEE Transactions on Device and Materials Reliability, 2008, 8, 332-343.	1.5	535
102	Investigation of High-Electric-Field Degradation Effects in AlGaN/GaN HEMTs. IEEE Transactions on Electron Devices, 2008, 55, 1592-1602.	1.6	110
103	Mechanisms of RF Current Collapse in AlGaN–GaN High Electron Mobility Transistors. IEEE Transactions on Device and Materials Reliability, 2008, 8, 240-247.	1.5	83
104	Characterization and Numerical Simulations of High Power Field-Plated pHEMTs. , 2008, , .		1
105	Radon alpha-ray detector based on a high-resistivity-silicon BJT and a low-cost readout electronics. , 2008, , .		2
106	Application of the BJT detector for simple, low-cost, and low-power alpha-particle detection systems. , 2007, , .		5
107	Recent development on triple well 130 nm CMOS MAPS with in-pixel signal processing and data sparsification capability. , 2007, , .		12
108	Proposal of a data sparsification unit for a mixed-mode MAPS detector. , 2007, , .		22

#	Article	IF	CITATIONS
109	A review of failure modes and mechanisms of GaN-based HEMTs. , 2007, , .		31
110	Development of deep N-well monolithic active pixel sensors in a CMOS technology. Nuclear Instruments and Methods in Physics Research, Section A: Accelerators, Spectrometers, Detectors and Associated Equipment, 2007, 572, 277-280.	0.7	9
111	Recent developments in 130 nm CMOS monolithic active pixel detectors. Nuclear Physics, Section B, Proceedings Supplements, 2007, 172, 20-24.	0.5	1
112	Monolithic integration of detectors and transistors on high-resistivity silicon. Nuclear Instruments and Methods in Physics Research, Section A: Accelerators, Spectrometers, Detectors and Associated Equipment, 2007, 579, 658-663.	0.7	5
113	Characterization and analysis of trap-related effects in AlGaN–GaN HEMTs. Microelectronics Reliability, 2007, 47, 1639-1642.	0.9	31
114	Fabrication, Characterization and Numerical Simulation of High Breakdown Voltage <code>pHEMTs.</code> , 2006, , .		2
115	Physical Investigation of High-Field Degradation Mechanisms in GaN/AlGaN/GaN HEMTS. , 2006, , .		3
116	Development of 130nm CMOS Monolithic Active Pixels with In-pixel Signal Processing. , 2006, , .		6
117	BJT-based detector on high-resistivity silicon with integrated biasing structure. Nuclear Instruments and Methods in Physics Research, Section A: Accelerators, Spectrometers, Detectors and Associated Equipment, 2006, 567, 285-289.	0.7	4
118	Performance evaluation of radiation sensors with internal signal amplification based on the BJT effect. Nuclear Instruments and Methods in Physics Research, Section A: Accelerators, Spectrometers, Detectors and Associated Equipment, 2006, 568, 217-223.	0.7	9
119	Current Collapse and High-Electric-Field Reliability of Unpassivated GaN/AlGaN/GaN HEMTs. IEEE Transactions on Electron Devices, 2006, 53, 2932-2941.	1.6	150
120	N–p–n bipolar-junction-transistor detector with integrated p–n–p biasing transistor—feasibility study, design and first experimental results. Semiconductor Science and Technology, 2006, 21, 194-200.	1.0	1
121	DC-to-RF dispersion effects in GaAs- and GaN-based heterostructure FETs: performance and reliability issues. Microelectronics Reliability, 2005, 45, 1585-1592.	0.9	7
122	Radiation-hard semiconductor detectors for SuperLHC. Nuclear Instruments and Methods in Physics Research, Section A: Accelerators, Spectrometers, Detectors and Associated Equipment, 2005, 541, 189-201.	0.7	55
123	Light Sensitivity of Current DLTS and Its Implications on the Physics of DC-to-RF Dispersion in AlGaAs–GaAs HFETs. IEEE Transactions on Electron Devices, 2005, 52, 594-602.	1.6	6
124	Surface-Related Drain Current Dispersion Effects in AlGaN–GaN HEMTs. IEEE Transactions on Electron Devices, 2004, 51, 1554-1561.	1.6	255
125	The Impact of Light on Current DLTS and Gate-Lag Transients of AlGaAs–GaAs HFETs. IEEE Electron Device Letters, 2004, 25, 517-519.	2.2	6
126	Experimental and numerical assessment of gate-lag phenomena in AlGaAs-GaAs heterostructure field-effect transistors (FETs). IEEE Transactions on Electron Devices, 2003, 50, 1733-1740.	1.6	29

#	Article	IF	CITATIONS
127	Radiation tolerance of epitaxial silicon carbide detectors for electrons, protons and gamma-rays. Nuclear Instruments and Methods in Physics Research, Section A: Accelerators, Spectrometers, Detectors and Associated Equipment, 2003, 505, 645-655.	0.7	100
128	Origin of hole-like peaks in current deep level transient spectroscopy of n-channel AlGaAs/GaAs heterostructure field-effect transistors. Journal of Applied Physics, 2003, 94, 5297.	1.1	16
129	Energetic and spatial localisation of deep-level traps responsible for DC-to-RF dispersion effects in AlGaAs–GaAs HFETs. Electronics Letters, 2003, 39, 1548.	0.5	2
130	Study on the origin of dc-to-RF dispersion effects in GaAs- and GaN-based beterostructure FETs. , 2003, , .		2
131	Impact of temperature on surface-trap-induced gate-lag effects in GaAs heterostructure FETs. Electronics Letters, 2003, 39, 810.	0.5	4
132	A novel silicon microstrip termination structure with all p-type multiguard and scribe-line implants. IEEE Transactions on Nuclear Science, 2002, 49, 1712-1716.	1.2	6
133	Physics-based explanation of kink dynamics in AlGaAs/GaAs HFETs. IEEE Electron Device Letters, 2002, 23, 383-385.	2.2	19
134	Physical investigation of trap-related effects in power HFETs and their reliability implications. IEEE Transactions on Device and Materials Reliability, 2002, 2, 65-71.	1.5	7
135	Impact of programming charge distribution on threshold voltage and subthreshold slope of NROM memory cells. IEEE Transactions on Electron Devices, 2002, 49, 1939-1946.	1.6	53
136	Investigation on the charge collection properties of a 4H-SiC Schottky diode detector. Nuclear Instruments and Methods in Physics Research, Section A: Accelerators, Spectrometers, Detectors and Associated Equipment, 2002, 476, 717-721.	0.7	31
137	Extraction of bulk generation lifetime and surface generation velocity in high-resistivity silicon by means of gated diodes. Nuclear Instruments and Methods in Physics Research, Section A: Accelerators, Spectrometers, Detectors and Associated Equipment, 2002, 477, 220-225.	0.7	6
138	Trap characterization in buried-gate n-channel 6H-SiC JFETs. IEEE Electron Device Letters, 2001, 22, 432-434.	2.2	4
139	Analytical model for the ohmic-side interstrip resistance of double-sided silicon microstrip detectors. IEEE Transactions on Nuclear Science, 2001, 48, 972-976.	1.2	3
140	Monolithic integration of Si-PIN diodes and n-channel double-gate JFET's for room temperature X-ray spectroscopy. Nuclear Instruments and Methods in Physics Research, Section A: Accelerators, Spectrometers, Detectors and Associated Equipment, 2001, 458, 275-280.	0.7	13
141	Improvement in breakdown characteristics with multiguard structures in microstrip silicon detectors for CMS. Nuclear Instruments and Methods in Physics Research, Section A: Accelerators, Spectrometers, Detectors and Associated Equipment, 2001, 461, 204-206.	0.7	14
142	Gate-lag effects in AlGaAs/GaAs power HFET's. Microelectronics Reliability, 2001, 41, 1585-1589.	0.9	0
143	Surface effects on turn-off characteristics of AlGaAs/GaAs HFETs. Electronics Letters, 2001, 37, 719.	0.5	4
144	Trap energetic and spatial localization in buried-gate 6H-SiC JFETs by means of numerical device simulation. IEEE Electron Device Letters, 2001, 22, 579-581.	2.2	1

#	Article	IF	CITATIONS
145	Charge preamplifier for hole collecting PIN diode and integrated tetrode N-JFET. IEEE Transactions on Nuclear Science, 2000, 47, 829-833.	1.2	12
146	Development of silicon microheaters for chemoresistive gas sensors. , 1999, 3680, 964.		1
147	Two-dimensional numerical simulation of edge-generated currents in type-inverted, p/sup +/-n single-sided silicon microstrip detectors. IEEE Transactions on Nuclear Science, 1999, 46, 1253-1257.	1.2	3
148	Gate oxide reliability improvement related to dry local oxidation of silicon. Microelectronics Reliability, 1999, 39, 181-185.	0.9	0
149	On the accuracy of generation lifetime measurement in high-resistivity silicon using PN gated diodes. IEEE Transactions on Electron Devices, 1999, 46, 817-820.	1.6	15
150	Study of breakdown effects in silicon multiguard structures. IEEE Transactions on Nuclear Science, 1999, 46, 1215-1223.	1.2	42
151	Optimization of TMAH etching for MEMS. , 1999, 3680, 969.		4
152	Silicon PIN radiation detectors with on-chip front-end junction field effect transistors. Nuclear Instruments and Methods in Physics Research, Section A: Accelerators, Spectrometers, Detectors and Associated Equipment, 1998, 417, 325-331.	0.7	16
153	Design and optimization of an npn silicon bipolar phototransistor for optical position encoders. Microelectronics Journal, 1998, 29, 49-58.	1.1	2
154	High-voltage operation of silicon devices for LHC experiments. Nuclear Instruments and Methods in Physics Research, Section A: Accelerators, Spectrometers, Detectors and Associated Equipment, 1998, 409, 139-141.	0.7	6
155	Development of a detector-compatible JFET technology on high-resistivity silicon. Nuclear Instruments and Methods in Physics Research, Section A: Accelerators, Spectrometers, Detectors and Associated Equipment, 1998, 409, 346-350.	0.7	5
156	Radiation effects on breakdown characteristics of multiguarded devices. IEEE Transactions on Nuclear Science, 1997, 44, 721-727.	1.2	23
157	Numerical analysis of ISFET and LAPS devices. Sensors and Actuators B: Chemical, 1997, 44, 402-408.	4.0	12
158	Modeling of light-addressable potentiometric sensors. IEEE Transactions on Electron Devices, 1997, 44, 2083-2090.	1.6	10
159	Si-PIN X-ray detector technology. Nuclear Instruments and Methods in Physics Research, Section A: Accelerators, Spectrometers, Detectors and Associated Equipment, 1997, 395, 344-348.	0.7	23
160	Forward and reverse characteristics of irradiated MOSFETs. IEEE Transactions on Nuclear Science, 1996, 43, 797-804.	1.2	4
161	Influence of impact-ionization-induced base current reversal on bipolar transistor parameters. IEEE Transactions on Electron Devices, 1995, 42, 1636-1646.	1.6	20
162	Design of an n-channel JFET on high-resistivity silicon for radiation-detector on-chip front-end electronics. Nuclear Instruments and Methods in Physics Research, Section A: Accelerators, Spectrometers, Detectors and Associated Equipment, 1995, 365, 473-479.	0.7	4

#	Article	IF	CITATIONS
163	FOXFET biased microstrip detectors: an investigation of radiation sensitivity. Nuclear Instruments and Methods in Physics Research, Section A: Accelerators, Spectrometers, Detectors and Associated Equipment, 1994, 342, 39-48.	0.7	11
164	Punch-through characteristics of FOXFET biased detectors. IEEE Transactions on Nuclear Science, 1994, 41, 804-810.	1.2	2
165	Prediction of impact-ionization-induced snap-back in advanced Si n-p-n BJT's by means of a nonlocal analytical model for the avalanche multiplication factor. IEEE Transactions on Electron Devices, 1993, 40, 2296-2300.	1.6	19
166	Extraction of DC base parasitic resistance of bipolar transistors based on impact-ionization-induced base current reversal. IEEE Electron Device Letters, 1993, 14, 431-434.	2.2	11
167	Degradation of silicon AC-coupled microstrip detectors induced by radiation. IEEE Transactions on Nuclear Science, 1993, 40, 2001-2007.	1.2	8
168	Extension of impact-ionization multiplication coefficient measurements to high electric fields in advanced Si BJT's. IEEE Electron Device Letters, 1993, 14, 69-71.	2.2	32
169	Radiation tolerance of the FOXFET biasing scheme for AC-coupled Si microstrip detectors. IEEE Transactions on Nuclear Science, 1993, 40, 1602-1609.	1.2	9
170	Experimental and numerical analysis of gate- and drain-lag phenomena in AlGaAs/InGaAs PHEMTs. , 0, , .		1